

A self-consistent kinetic modeling of a 1-D, bounded, plasma in equilibrium

MONOJOY GOSWAMI and H RAMACHANDRAN

Institute for Plasma Research, Bhat, Gandhinagar 382 428, India

Abstract. A self-consistent kinetic treatment is presented here, where the Boltzmann equation is solved for a particle conserving Krook collision operator. The resulting equations have been implemented numerically. The treatment solves for the entire quasineutral column, making no assumptions about λ_{mfp}/L , where λ_{mfp} is the ion-neutral collision mean free path and L the size of the device. Coulomb collisions are neglected in favour of collisions with neutrals, and the particle source is modeled as a uniform Maxwellian. Electrons are treated as an inertialess but collisional fluid. The ion distribution function for the trapped and the transiting orbits is obtained. Interesting findings include the anomalous heating of ions as they approach the presheath, the development of strongly non-Maxwellian features near the last λ_{mfp} , and strong modifications of the sheath criterion.

Keywords. Plasma kinetic equation; ion-neutral collision; presheath.

PACS Nos 52.65; 52.40H; 72.30; 52.50D; 52.20

1. Introduction

The nature of the collisional presheath of a plasma has been an elusive matter for investigation. It is conventionally regarded as that region of the plasma where ion inertia effects are significant yet where the plasma is still quasineutral [1,2]. The conventional understanding also regards the collisional presheath to be a boundary layer between the transport dominated central region and the sheath proper [1]. In an earlier work [9], the authors investigated both these issues using a fluid approach that retained both collisions and inertia throughout the plasma column and obtained equilibrium profiles in response to a uniform plasma source. It was found that while the presheath did develop and was localized to the last few mean-free-paths, λ_{mfp} , significant deviations appeared as compared to ideal presheath theories [5].

One of the shortcomings of the earlier study was the assumption of a nearly Maxwellian distribution for ions in the presheath. This is implicit in any fluid approach. However, it is unlikely to be valid. Another shortcoming was that the ions were assumed to satisfy an adiabatic equation of state throughout the plasma column. This assumption is manifestly false in the interior of the plasma, and possibly questionable even in the edge.

The current investigation is therefore an attempt to investigate the importance of these fundamental issues. This paper reports on the findings of a kinetic code that retains collisions and sources, models the entire quasineutral portion of the plasma column without

resorting to boundary layer techniques and obtains equilibrium profiles for systems as large as $200 \lambda_{mf}$ in extent. This code is still in its final development, but the findings are compelling enough to warrant this report. The equation of state is found to be significantly different from that assumed in fluid theories. The ion distribution is found to be dramatically non-Maxwellian in the presheath. And the profiles in the vicinity of the wall show a different singularity from the square-root singularity predicted by all prior studies.

The next section briefly discusses the equations that are implemented. Section 3 then details the numerical procedure. Section 4 concludes the paper by presenting the findings of the code and discusses their implications.

2. A kinetic formulation

Figure 1 presents the geometry assumed in this study. A non-plasma source (eg., UV light) that creates plasma uniformly in a length $-L < x < L$ is assumed to be present. The boundaries of the plasma at $-L$ and L are assumed to be perfectly absorbing. Inside the plasma ion-neutral collisions are assumed to dominate i.e. the plasma is weakly ionized. The collisional model used for ion-neutral collisions cannot be used to describe electron collisions, since electrons isotropize via collisions with neutrals and thermalize through collisions with other electrons. However, due to the presence of electron confining potentials in the sheath, electrons have a long residence time in the plasma and are essentially thermalized. They may therefore be modelled as a collisional fluid. The collisional Vlasov equation for the ions in steady state becomes

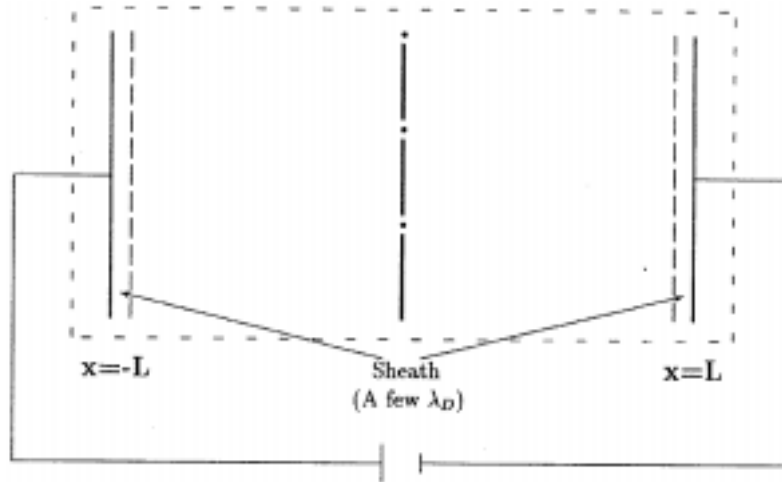


Figure 1. Schematic of the geometry assumed in this paper. A 1-dimensional column of plasma is assumed present between two fully absorbing walls. A uniform source is assumed present throughout the region.

$$v \frac{\partial f_i}{\partial x} - \frac{e}{m_i} \frac{\partial \phi}{\partial x} \frac{\partial f_i}{\partial v} + \nu_i(v) f_i = S(v) + \nu_i(v) g(v, T_0), \quad (1)$$

where $S(v)$ is the uniform source term and collisions have been modeled by a particle conserving Krook operator, and $g(v, T_0)$ is a Maxwellian suitably normalized to conserve particles (but not momentum or energy). The walls do not inject particles into the system, which yields the boundary condition for the problem,

$$f_i(-L, v > 0) = f_i(+L, v < 0) = 0. \quad (2)$$

Equation (1) may be solved by the method of characteristics. In Lagrangian coordinates with

$$\dot{x} = v \quad \text{and} \quad \dot{v} = -\frac{e}{m_i} \frac{\partial \phi}{\partial x}. \quad (3)$$

Equation (1) becomes for the Lagrangian phase space density, $\tilde{f}_i(\tau_i; x_0, v_0)$,

$$\frac{d\tilde{f}_i}{d\tau_i} + \nu_{0i}(v(\tau_i)) \tilde{f}_i(\tau_i) = S(x(\tau_i), v(\tau_i)) + \nu_{0i}(\tau_i) g(v(\tau_i), T_0), \quad (4)$$

where the dependence on x_0 and v_0 has been suppressed for clarity. The solution yields,

$$\begin{aligned} \tilde{f}_i(\tau_i; x_0, v_0) = & \int_{\tau_{i0}}^{\tau_i} \nu_i d\tau'_i \left[gn_i + \frac{S}{\nu_i} \right] (\tau'_i) e^{-\nu_i(\tau_i - \tau'_i)} \\ & + f_i(x_0, v_0) e^{-\nu_i(\tau_i - \tau_{i0})}. \end{aligned} \quad (5)$$

f thus approaches the local value $(gn_i + S/\nu_i)$ averaged over a λ_{mfip} . Since in one collision time the distribution decays to gn_i , either significant density needs to be injected in that time or else the plasma must vary strongly inside the λ_{mfip} window to prevent equilibration.

The collisional model used in eq. (1) is based on a BGK [4] type of treatment. It is quite suitable for describing collisions between ions and equally massive neutrals which consist of large angle scattering that relax momentum and energy at equal rates.

The collision frequency has been assumed in this paper to be a linear function of velocity,

$$\nu(\xi, v) = \nu_0 \left(1 + \frac{v}{\bar{v}_0} \right) \quad (6)$$

where $\bar{v}_0 = \sqrt{T_0/m_i}$ is the thermal velocity of the source particles and ν_0 is the ion-neutral collision frequency for thermal ions. This model yields a constant λ_{mfip} for fast ions, consistent with the idea of scattering off a random collection of stationary scattering points, while it yields a constant ν for slow ions, consistent with the idea of collisions experienced by a stationary particle in an ideal gas. For this treatment, ν_0 has been assumed independent of position.

Riemann [6] has used the constant mean-free-path model for the ion-neutral collisions to model Boltzmann equation for charge exchange collisions with cold neutrals. In the same paper ([6], appendix A) he discussed the constant collision frequency case which has not been used. The constant collision frequency may be a reasonable approximation in low fields [7], where the relative velocity of the collision partners does not differ essentially from the thermal neutral velocity. Although Emmert [8] has considered collision frequency that is a function of speed, this model has been used in ion-ion Coulomb collisions. The model assumes $\nu(v) \sim |v|$, which is a very poor approximation in the limit $|v| \rightarrow 0$.

Our collision model, eq. (6), is a reasonable approximation for both the limits i.e., for small as well as large thermal velocities. It captures the physics for both large and small thermal velocities.

The characteristics defined by eq. (3) correspond to single particle ion orbits in a collisionless system. Since the ambipolar electric field that develops serves to retard the electrons and accelerate the ions to the walls, all these orbits eventually intersect the boundaries twice. The Lagrangian time coordinate is normalized by setting the time at which the orbit originates from the walls to be zero, i.e., $\tau_{i0} = 0$. Then eq. (5) yields

$$\begin{aligned}
 f_i(x, v) &= \tilde{f}_i(\tau_i; \pm L, v_W) \\
 &= \int_0^{\tau_i} \nu_i d\tau'_i \left[gn_i + \frac{S}{\nu_i} \right] e^{-\nu_i(\tau_i - \tau'_i)} + f_i(\pm L, v_W) e^{-\nu_i \tau_i} \\
 &= \int_0^{\tau_i} \nu_i d\tau'_i \left[gn_i + \frac{S}{\nu_i} \right] e^{-\nu_i(\tau_i - \tau'_i)} \tag{7}
 \end{aligned}$$

since the walls are assumed to be non-emissive.

The orbits still fall into two classes, however. Some of the orbits have the energy to cross over the central potential barrier and reach the opposite wall. These are designated in this paper as ‘transiting’ orbits. Other orbits are reflected by the potential and have a turning point, x_0 . They then reverse direction and come back to the same wall from which they originated. These orbits are designated as ‘trapped’. The solution of these ‘trapped’ orbits requires use of the continuity conditions

$$\lim_{x \rightarrow x_0^-} f_i(x, v) = \lim_{x \rightarrow x_0^-} f_i(x, -v) \tag{8}$$

for orbits originating at $x = -L$ and

$$\lim_{x \rightarrow x_0^+} f_i(x, v) = \lim_{x \rightarrow x_0^+} f_i(x, -v) \tag{9}$$

for orbits originating at $x = L$. These conditions are obtained by integrating eq. (7) in *time* from just before to just after reaching the turning point. There is one class of orbits, however, that falls into neither category. These are the orbits that are barely reflected by

the potential barrier, or are barely transiting. For these orbits, the continuity conditions eq. (8) and eq. (9) are not well satisfied. However, eq. (7) may be rewritten as

$$f_i(x, v) = \int_{\pm L}^x \frac{dx'}{\lambda_{\text{mfp}}(x')} \left[gn_i + \frac{S}{\nu_i} \right] e^{-\int_{\pm L}^{x'} \frac{dx''}{\lambda_{\text{mfp}}(x'')}}. \quad (10)$$

Since $\lambda_{\text{mfp}} \propto v$ as $v \rightarrow 0$ for the chosen collision operator, and $v \propto x$ near the potential peak, f_i asymptotes to the local value of the quantity in square brackets, $gn_i + S/\nu_i$ at the turning point. Thus the continuity of f_i is assured now, not by residence time considerations, but by the continuity of $gn_i + S/\nu_i$.

An equilibrium treatment of an ambipolar plasma always yields monotonic density and potential profiles. However, even a very weak level of noise will disrupt the monotonicity of potential at $x = 0$. The result is the appearance of transient regions of trapping potential. The orbits in such a system will then become very complex. However, the trapping width is small, which implies that the orbits involved have $v \sim 0$ in this region. Thus, the strong collisional effects coupled with the dynamical chaos expected in such regions of phase space will serve to wash out any special effects they might otherwise produce.

The region under consideration is quasineutral i.e., $n_e \approx n_i = n$. The potential can therefore be obtained from the electron equation. Electrons are treated as a collisional, inertialess fluid, and satisfy

$$0 = -enE_x - dp_e/dx - m_e n \nu_{en} u_e, \quad (11)$$

where $p_e = nT_e$ is the electron pressure, $E_x = -d\phi/dx$ is the electric field, m_e is the mass of the electrons, u_e is the fluid velocity of the electrons and $\nu_{en} = \nu_{e0} u_e / \bar{v} = \nu_0 \sqrt{T_e m_e / T_0 m_i} u_e / \bar{v}$ is the electron-neutral collision frequency for electrons. In this treatment, external currents are assumed absent, and so

$$u_e(x) = u_i(x) = u(x) = \int_{-\infty}^{\infty} f_i(x, v) v dv \quad (12)$$

holds. Assuming isothermal electrons, eq. (11) yields the normalized potential, $\psi = -e\phi/T_e$, in terms of the density and velocity moments:

$$\psi(x) = \psi(0) + \ln \left(\frac{n(x)}{n(0)} \right) + \nu_0 \sqrt{\frac{m_e m_i}{T_e T_0}} \int_0^x v(x') dx'. \quad (13)$$

This completes the system of equations to be solved.

3. Numerical procedures

The problem is parametrized by a few parameters. These include the mass ratio for ions, the ratio of electron to source temperatures T_e/T_0 and the value of λ_{mfp} for thermal ions.

The strength of the particle source S is automatically determined by the edge density, and its velocity distribution is assumed to be the same Maxwellian that describes the neutral particles. For the results presented in this paper, the mass ratio was fixed at 1836.

The procedure of obtaining the solution involved the following steps:

1. Start with the parameters for the problem. The system is meshed in x by a non-uniform mesh with points concentrated in the last λ_{mfp} nearest the walls.
2. Start with guessed profiles for density and flow velocity.
3. For the guessed profiles, the potential profile is obtained.
4. A corresponding mesh is created in E , the energy coordinate. The minimum energy of the orbits is determined by the potential, while the maximum energy is determined by obtaining upper bounds for $f(x, v)$ from eq. (7).
5. Equation (7) is now solved along each characteristic. Turning points and separatrix orbits are handled as discussed in the previous section.
6. The resulting distribution functions are now integrated to obtain their density and velocity moments.
7. These are compared with the guessed profiles for convergence. If convergence is not reached, a revised guess is made and the procedure is repeated from step 3.

While these converged profiles are self-consistent, they suffer from an important deficiency. The form of the collision operator used is not particle conserving except for a constant collision frequency. Thus, the correct equation to solve should have been

$$f_i(x, v) = \int_0^{\tau_i} \nu_i d\tau'_i \left[g\tilde{n}_i + \frac{S}{\nu_i} \right] e^{-\nu_i(\tau_i - \tau'_i)}, \quad (14)$$

where \tilde{n}_i is an adjusted density that achieves particle conservation. Since the actual density was used in the runs reported in this paper, the source of particles is modified from the explicit source $S(v)$. This is found to have a significant effect on the solutions as discussed in the next section.

One other issue is the uniqueness of the solutions. In a real plasma, it is known that the quasineutral plasma develops flows approaching ion-acoustic velocities at the sheath edge, which are then evolved further into the super-ion-acoustic regime in the sheath itself. In a fluid treatment, this is an explicit requirement. In the kinetic code, no such requirement is made. The procedure seeks its own solutions which are then to be examined for the presence of the equivalent of the Bohm condition.

4. Results and discussion

The procedure described in the previous section was carried using solutions from a previously developed fluid code [9]. Since the problem is nonlinear in character, an iteration

scheme was employed to achieve convergence. Contrary to expectations, convergence was achieved with a simple-minded iteration of the form

$$\mu_{i+1}(x) = \alpha\mu_i(x) + (1 - \alpha)\mu_i^{\text{iter}}(x), \quad (15)$$

where μ_i are the guessed density and velocity profiles for the i th iteration, μ_i^{iter} the density and velocity profiles obtained in step 6 of the procedure described in the previous section, and μ_{i+1} the revised guesses for step $i + 1$. The maximum, absolute error in the profiles were found to drop three orders in the first ten iterations, before stagnating. Slow improvement in error continued to occur upto a hundred iterations, where the inaccuracies of the procedures prevented further improvement. All the profiles were accurate to four significant digits (which was also the cumulative accuracy of the various numerical procedures employed.)

Density and velocity profiles are shown in figure 2, for a case of $T_e = T_i$ and $\lambda_{\text{mfp}}/L = 0.01$. The profile of the density, normalized to the edge density is presented in figure 2a. For this value of λ_{mfp}/L , the central density is predicted by ambipolar theory to be 25. Numerically it is found to be double this number. This is easily understood as a

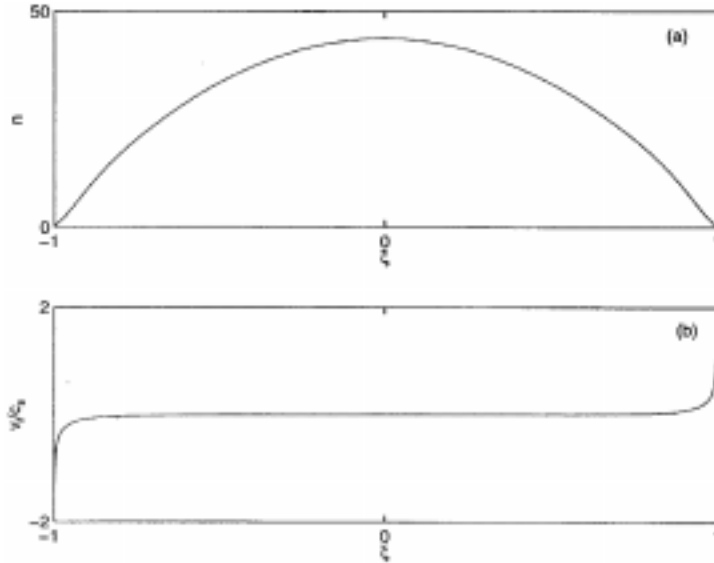


Figure 2. Density and velocity profiles obtained from the numerical code, for the case of $\lambda_{\text{mfp}}/L = 0.01$ and $T_0/T_e = 0.5$. (a) The density profile, normalized to the edge density. Since the system is many λ_{mfp} in length, the central density is considerable. (b) The velocity profile, normalized to $c_s = T_e/m_i$. As seen in the figure, the profiles achieve an edge velocity in excess of unity. The value achieved is close to the predicted value of $\sqrt{1 + \gamma T_0/T_e}$.

consequence of the velocity dependence of the collision operator. The value of ν_0 in the code is obtained from this value of λ_{mfp}/L . However, thermal particles experience an equal contribution from the velocity dependent term in eq. (6). Thus the average collision frequency that appears in the momentum equation is double the nominal value, doubling the central density.

The velocity profile shown in figure 2b is very flat in the bulk region, as expected. In the sheath region, the velocity rises to a value of $1.53 \sqrt{T_e/m_i}$. The fluid prediction for this profile, $\sqrt{T_e + \gamma T_i/m_i} = 2.0 \sqrt{T_e/m_i}$, is much higher. This indicates that either the profiles have not reached the sheath as yet, or the fluid expression for the Bohm velocity is an error. An improved expression has been obtained by the authors, namely,

$$\frac{m_i c_s^2}{T_e} = 0.5 + 0.5 \sqrt{1 + 12 \frac{T_i}{T_e}}. \quad (16)$$

This expression yields a prediction of $1.52 \sqrt{T_e/m_i}$, very close to the observed value for this case.

The Maxwellian-ness of the distribution is explored in figure 3. The square-root of the logarithm of the distribution function at a point close to the left edge is plotted versus velocity in the drift frame (plus symbols). Thus, if truly Maxwellian, a pair of straight lines should result. The dashed lines correspond to a Maxwellian with the locally measured temperature. The two dotted lines correspond to the source distribution function (a Maxwellian in the laboratory frame), suitably scaled. As is clear from this graph, the slow particles of the distribution function have equilibrated to a drifting Maxwellian, but the tail particles lie on the source contours, indicating that they are yet to equilibrate.

An alternate understanding of figure 3 is possible. The slowly moving particles have a short λ_{mfp} and thus equilibrate to the local distribution. However, the tail particles have larger λ_{mfp} and attempt to equilibrate to a space averaged distribution. In the edge region where the distribution is varying sharply, this space-averaged distribution is quite different from the local one. In any event, the distribution is clearly far from equilibrium.

One interesting feature of this figure is the anisotropy in the positive and negative velocity tail distributions. While both fit to a stationary Maxwellian distribution, the negative velocity tail is a thousand times the strength of the positive tail. This is a consequence of the spatial location. This location is very close to the left wall. Thus positive velocity particles are very few in number, given that the wall is non-emissive. The negative velocity particles come from the bulk and are therefore numerous. Indeed, they are three times more numerous than required by the locally present source, clearly an effect of the non-local response of the kinetic system.

The temperature profile of a case with $\lambda_{\text{mfp}}/L = 0.01$ and $T_0/T_e = 0.5$ is presented in figure 4a (The parameters were chosen to enhance the features discussed here). As expected, the temperature is very flat in the interior of the plasma column, confirming the isothermal nature of bulk plasma. However in the last few λ_{mfp} , the temperature is seen to rise sharply. This can be understood as follows. Near the edge the plasma develops a strong flow velocity. The intermediate region, where the wall is still a collisional length

away, but the drift velocity is appreciable sees a new effect. The source continues to inject a distribution with zero drift. However, in the frame of the drifting plasma, this injected source appears to be a drifting Maxwellian. Thus, the total energy per particle injected is $m\bar{v}^2/2 + m\bar{v}_d^2/2$. Since this exceeds $\kappa T_0/2$, the R.M.S. width of the distribution increases. Thus the plasma is actually heated by the source.

Once the particles are close to the wall, however, the adiabatic cooling from the strong acceleration experienced due to the presheath electric field overwhelms this heating effect and the temperature comes plummeting down. The distribution presented in figure 3 was located in this region.

Figure 4b presents the effective value of γ computed from the profiles. γ is seen to rise sharply in the last λ_{mfp} from below unity over 5, which is even higher than the adiabatic value. This suggests that fluid treatments that assume an equation of state are likely to be in error in this region. Of course, the strongly non-Maxwellian nature of the distribution function in this region makes all fluid treatments of this region questionable.

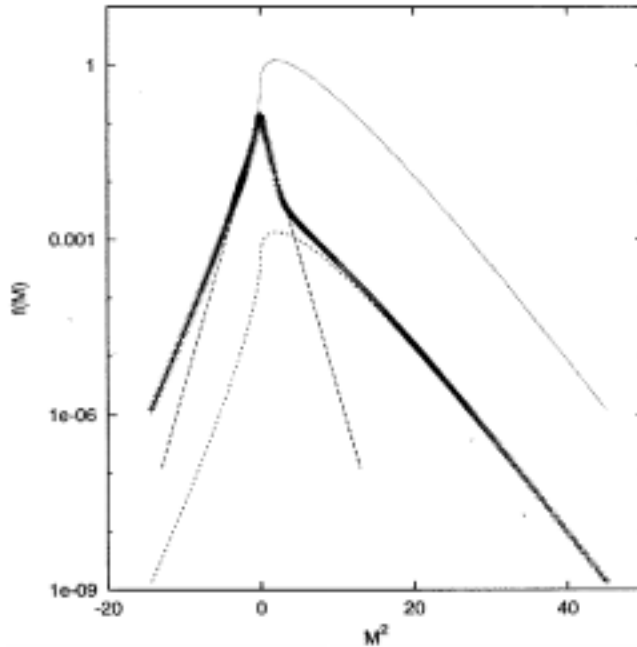


Figure 3. The Maxwellian-ness of the distribution function is shown for the case $\lambda_{mfp}/L = 0.01$ and $T_0/T_e = 1.0$. The logarithm of the distribution function is plotted versus the square of the velocity in the drifting frame. For a Maxwellian plot, this results in a straight line. The plus symbols are the distribution very near to the left edge of the plasma. The dashed line correspond to a Maxwellian with the locally measured temperature. The two dotted lines correspond to the suitably scaled source distribution function.

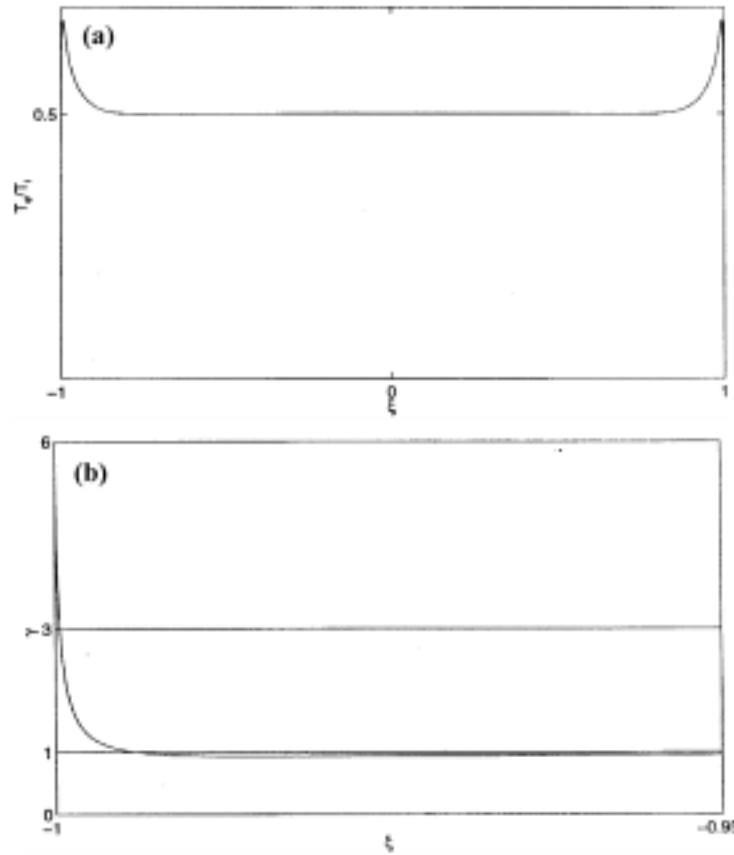


Figure 4. (a) The temperature profile for a case of $\lambda_{mfp}/L = 0.01$ and $T_0/T_e = 0.5$. The ion temperature is seen to equilibrate to the source temperature in the middle of the system, but is seen to rise strongly in the edge regions. It finally drops dramatically in the presheath itself due to adiabatic cooling and reaches approximately the source temperature at the edge. (b) The value of γ determined from $T_i \propto n^{\gamma-1}$ for the same run. The value of γ is less than unity in the bulk since the temperature rises even as the density falls. However, in the presheath, γ rises to exceed its adiabatic value of 3.

The issue of the uniqueness of solutions was one of the issues to be explored. To address this issue, different initial seed profiles were used and the program iterated till it converged. The code was observed to converge to the same profile regardless of initial condition. Some initial conditions, such as a parabolic profile as expected from ambipolar theory, did not converge. However, all seed profiles that did converge, converged to a unique profile. If the converged profile were not a profile containing the presheath singularity, different seeds should have converged to different solutions. Thus this uniqueness suggests strongly that the solution is the one that will match to the sheath.

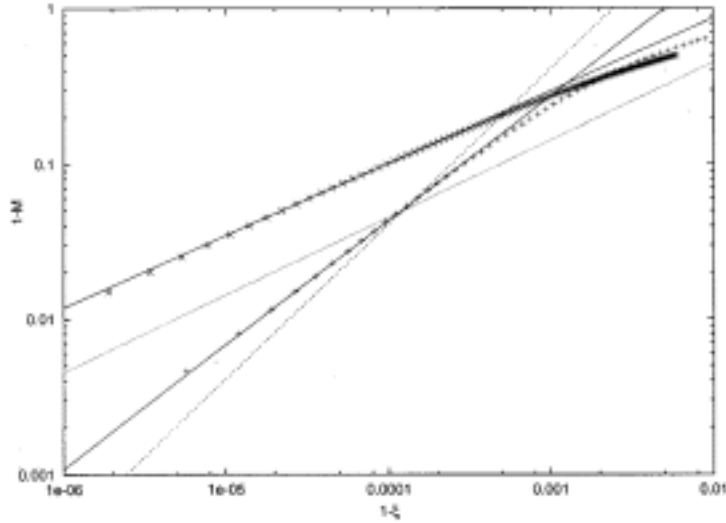


Figure 5. The velocity profile is presented at the last λ_{mfp} to diagnose the singularity at the sheath edge. The plus symbols are the results from the code. The solid line passing through the plus symbols correspond to a curve $(1 - M) \propto (1 - \xi)^{0.8}$. The dotted line corresponds to $(1 - M) \propto \sqrt{1 - \xi}$ and the dashed line corresponds to $(1 - M) \propto (1 - \xi)$. Clearly this shows a singularity, although not of the square root type.

To explore the presence or absence of a singularity at the sheath edge, figure 5 presents the velocity profile in the last λ_{mfp} . If a singularity is present, then $1 - M$ should be some power of $1 - \xi$ near the edge. The plus symbols are the results from the code. The solid line passing through these symbols corresponds to a curve $1 - M \propto (1 - \xi)^{0.8}$. The dotted straight line in the figure corresponds to $1 - M \propto \sqrt{1 - \xi}$ while the dashed straight line corresponds to $1 - M \propto 1 - \xi$. Clearly, a singularity is present, and equally clearly it is not a square-root type of singularity.

The proper understanding of this result is complicated by the presence of a non-particle conserving collision operator. Effectively, this means that an inhomogeneous source is present. Following the derivation presented in [9], the equivalent fluid equation for a collisional plasma column with an inhomogeneous source is given by

$$\frac{dM}{d\xi} - \frac{\alpha M^2 \left(1 + M/\overline{M}\right)}{1 - M^2} = \frac{S(\xi)M}{\int_0^\xi S d\xi'} \frac{1 + M^2}{1 - M^2}, \quad (17)$$

where M is the velocity scaled to c_s , the ion-acoustic speed, $\overline{M} = \overline{v}_i/c_s$ is the ion thermal velocity scaled to c_s , $\overline{M}/\alpha = \lambda_{\text{mfp}}/L$ is the mean-free-path scaled to system length and the external current is assumed to be zero. For a very collisional system such

as studied in this paper, the integrated source varies little in the presheath. The effective source was observed to be constant (though negative, i.e., a sink) in the presheath region. This equation can therefore be rewritten in the vicinity of the edge as,

$$\frac{dM}{d\xi} = \frac{\alpha M^2 \left(1 + M/\overline{M}\right)}{1 - M^2} + \beta M \frac{1 + M^2}{1 - M^2}, \quad (18)$$

where $\beta = S(\xi)/\int_0^\xi S d\xi'$ is the roughly constant source term. Equation (18) is easily reduced to quadrature, is plotted in figure 5 as crosses. The solid straight line through the crosses is a best fit curve of the type $1 - M \propto \sqrt{1 - \xi}$. This confirms the presence of a square root singularity in the fluid treatment, even with an inhomogeneous source as present here.

The deviation between kinetic and fluid results has yet to be confirmed by systematic study and is a preliminary result. However, it is clear from the runs to date that the singularity is far weaker than it is predicted to be in fluid treatments. No understanding of this difference in behaviour between fluid and kinetic treatments is available at the current time.

To summarize, this paper reports on a self-consistent kinetic analysis of a bounded plasma in equilibrium. The numerical analysis has been carried out without using boundary layer techniques, to investigate the nature of presheath and the validity of conventional treatments. Findings include large modifications in the sheath criterion as well as the nature of the sheath singularity, heating of the distribution in the edge regions and the development of strong non-Maxwellian tails in the presheath region. Further investigation of these findings are in progress, to pin down the precise nature of the deviations from the conventional understanding of edge plasma behaviour in plasma columns.

References

- [1] K B Persson, *Phys. Fluids* **5**, 1625 (1962)
- [2] P N Hu and S Ziering, *Phys. Fluids* **9**, 2168 (1966)
- [3] D Bohm, in *The characteristics of electrical discharges in magnetic fields* edited by A Guthrie and R K Walkerling (McGraw Hill, NY, 1949) ch. 3, p. 90
- [4] P L Bhatnagar, E P Gross and M Krook, *Phys. Rev.* **94(3)**, 511 (1954)
- [5] K-U Riemann, *J. Phys.: Appl. Phys.* **D24**, 493 (1991)
- [6] K-U Riemann, *Phys. Fluids* **24(12)**, 2163 (1981)
- [7] E W McDaniel and E A Mason, *The mobility and diffusion of ions in gases* (Wiley, New York, 1973) ch. 5, 6 and 7
- [8] J T Scheuer and G A Emmert, *Phys. Fluids* **31(6)**, 1748 (1988)
- [9] Monojoy Goswami and H Ramachandran, *Phys. Plasmas* **6(9)**, 4522–32 (1999)